EFF-Doc-614

NUCLEAR SCIENCE AND ENGINEERING: 126, 176–186 (1997)

Gamma and Neutron Dosimetry Using CaF_2:Tm Thermoluminescent Dosimeters for Fusion Reactor Shielding Experiments

M. Angelone, P. Batistoni, M. Pillon, and V. Rado

Associazione Euratom-ENEA sulla fusione, Centro Ricerche Frascati C.P. 65, 00044 Frascati, Rome, Italy

and

A. Esposito

Istituto Nazionale Fisica Nucleare, Laboratori Nazionali di Frascati Via E. Fermi 44, 00044 Frascati, Rome, Italy

Received April 12, 1996
Accepted November 18, 1996

Abstract – *TLD-300 (CaF_2:Tm) dosimeters were used to measure the absorbed dose in an experimental assembly simulating the shield and the superconducting coils of a fusion reactor irradiated by 14-MeV neutrons. The shield was formed by plates of Type 316 stainless steel and by a water-equivalent material (Perspex), while a second block made of Type 316 stainless steel and copper plates simulated the superconducting coils of the tokamak. Since the TLD-300 shows two main peaks, one of which is more sensitive to neutrons, the neutron and gamma doses were separated using the two-peak method. The resulting absorbed neutron dose was 30% of the total in positions close to the neutron source, while its contribution was negligible (<7%) in the superconducting coils. The total dose level to be studied ranged from a few tens of micrograys to 10 Gy. Because the latter value was expected to be out of the linear response range for the TLD-300, the supralinear effects for the TLD-300 were studied as well as its sensitivity to determine the possibility of its use for doses as low as 10 μGy. Since the detector background can introduce an uncertainty of less than ±10%, the measurement of very low doses was performed with a total error lower than ±15%.*

I. INTRODUCTION

The International Thermonuclear Experimental Reactor (ITER) project[1] represents the major effort in the field of thermonuclear fusion. Many scientific as well as technological challenges are to be faced by the ITER project. Due to the intense emission of 14-MeV neutrons produced by the $T(d,n)^4He$ fusion reaction, one of these challenges is the proper definition of the performances and another is the design of the tokamak's shield blanket. It is well known that the 14-MeV neutrons carry, as kinetic energy, most of the fusion energy that is thus deposited into the structures surrounding the plasma vacuum vessel, mainly via neutron-induced (n,x) nuclear reactions. Prompt gamma rays are also produced by the neutron-induced nuclear reactions. Optimization of the shielding performances is a fundamental task of the engineering design activities of the ITER project. Together with the definition of the relevant neutronic properties of the shield, evaluation of the nuclear heating profiles generated inside this structure is becoming more important. The gamma-ray heating and the neutron absorbed dose near and inside the superconducting coils are key parameters to be evaluated for the good performance of a fusion reactor. Calculational techniques for the tokamak's shield-blanket design, mainly borrowed from fast nuclear reactor activities, are available for the absorbed-dose calculation, but until now they have not been thoroughly compared with experimental data. Measured

heating rates are thus required to provide direct insight about the quality of the available calculational tools.

In this paper we report the experimental results for absorbed dose measurements obtained in an assembly simulating the shield and the coils of a fusion reactor such as ITER. The experiment was carried out at the 14-MeV Frascati neutron generator[2] (FNG) of ENEA Frascati. In the FNG, which is a linear accelerator, a beam of deuterons (up to 1 mA) is accelerated to 300 keV onto a titanium tritide target. The tritium is adsorbed on a 4-μm-thick titanium layer deposited over a 1-mm-thick copper cup. Each target contains 37 GBq of tritium. The 14-MeV neutrons (up to 1.0×10^{11} n/s) are thus generated by the deuterium-tritium nuclear fusion reaction.

This paper deals mainly with the dosimetric aspect of the absorbed-dose measurements inside the shield, including the effort performed to separate the neutron and gamma dose using thermoluminescent dosimeters (TLDs). Nuclear heating was measured by TLD-300 (CaF_2:Tm) dosimeters.[3] A comparison with the calculated (neutron and gamma) doses, obtained via Monte Carlo calculation using the MCNP code[4] and the European Fusion File[5] (EFF) for the cross sections, is also reported.[6] The TLDs were chosen because they are small, sensitive, and easy to use. They have a broad linear response range, the ability to separate neutron and gamma doses for a certain kind of detector, and good reproducibility and are in an advanced state of development.

The TLD-300s are widely used in health physics and radiotherapy, mainly in gamma-neutron mixed fields.[7,8] We believe that this is the first attempt to use the TLD-300s in this kind of experiment and to separate the neutron and gamma doses experimentally.

II. THE EXPERIMENTAL ASSEMBLY

The experimental assembly is illustrated in Fig. 1. The shielding block consisted of nine 1- × 1-m, 5-cm-thick Type 316 stainless steel slabs, alternated with 2-cm-thick plates of water-simulating materials (Perspex) for a total thickness of 61 cm. The volumetric ratio of water to Type 316 stainless steel (30 and 70%, respectively) is that expected for a typical shield of a fusion reactor such as ITER. This block was followed by a 30-cm-thick block of copper and 2-cm-thick Type 316 stainless steel plates, simulating a superconducting magnetic coil. The assembly was located in the large FNG hall on a tower 4 m from walls, roof, and floor and at 5.8 cm from the FNG target.

In the experiment, the TLD-300s measured the absorbed dose in selected positions inside the Type 316 stainless steel and copper plates and throughout the two blocks. The output of the experiment is a comparison of the experimental data with the results of a transport calculation. For a better understanding of the results, this comparison uses absolute data normalized to one source neutron. This is straightforward for the Monte Carlo calculation, but it requires the absolute neutron emission of the FNG neutron source to normalize the experimental data. The FNG neutron emission is absolutely measured by means of the associated alpha-particle method.[9] A silicon surface detector (SSD) is located at 179.1 deg with respect to the beam line at a distance $L = 1820 \pm 5$ mm. A collimator [$\Delta\Omega = (3.147 \pm 0.018)10^{-7}$ sr] is also used to reduce the solid angle seen by the detector. The results furnished by the SSD were extensively calibrated against other detectors (fission chambers and activation foils) and methods (Monte Carlo calculation). This calibration is reported in Ref. 10. A total uncertainty of $\pm 2\%$ at 1σ (standard deviation) is obtained[10] for the FNG's absolute neutron emission.

III. SELECTION, SENSITIVITY, AND CALIBRATION OF THE TLD-300

The TLD-300 (CaF_2:Tm) phosphors match several properties such as high sensitivity, the possibility to separate gamma and neutron doses, and finally a medium effective atomic number ($Z_{eff} = 16.2$). These properties make the TLD-300 suitable for use in the mixed neutron and gamma fields to be investigated in our experiment as well as in a heavy medium such as a stainless steel shield. To expand further, according to Tanaka and Sasamoto,[11] an absorbed dose in a TLD

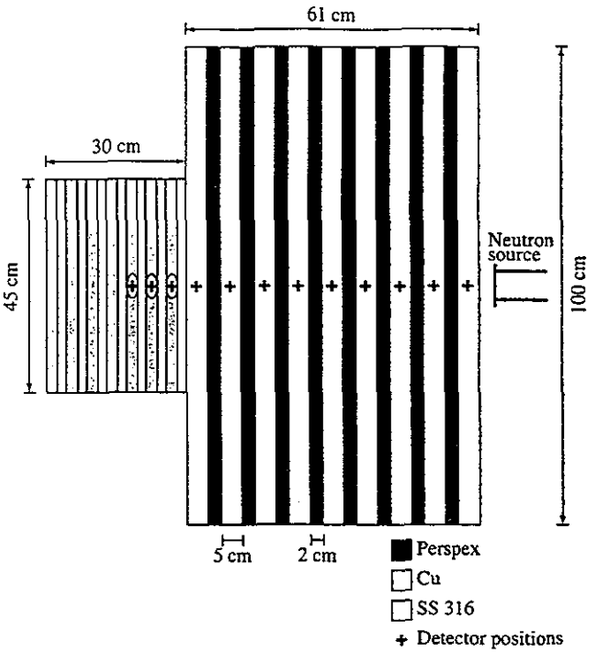

Fig. 1. Experimental assembly.

overestimates that in the surrounding medium with an atomic number smaller than that of the TLD, while it underestimates for the opposite case. In Ref. 11 it is also shown that the measured dose of TLD increases monotonically with the atomic number. In this sense, the TLD-300 with the reported Z_{eff} value is more suitable for use in the stainless steel shield than TLDs having a smaller Z_{eff} (e.g., LiF).

III.A. Selection of TLD-300

The TLD-300s used in this work were 3.2- × 3.2-mm, 0.9-mm-thick chips.[a] A group of 250 phosphors was used. The TLD reading was taken with an automatic reader[b] that uses nitrogen gas flow to clean up the heating chamber while the detector is heated by planchets. The heating ramp was 10°C/s, and the maximum reading temperature was 350°C. After reading, the TLD-300s were annealed in an oven at 400°C/h.

A typical thermoluminescent (TL) signal as a function of reading time for a TLD-300 irradiated with a ^{60}Co gamma ray is illustrated in Fig. 2. Three peaks are evident at 80, 150, and 240°C. A detailed study of the TLD-300 glow curve is reported elsewhere.[12,13] As in the literature, we label these peaks 2, 3, and 5 (see Fig. 2). It is also known that peaks 3 and 5 show different sensitivities to high linear energy transfer (LET) particles,[14] leading to the possibility of using these peaks to separate the neutron and gamma doses.[15,16] Peak 2 is generated by shallow trapped electrons and shows a nonnegligible fading ($T_{1/2}$ = 15 h). This leads to the reduction of the measured signal whenever the measurements are performed with some delay with respect to the irradiation. To avoid any problem with peak 2, it was eliminated by a preheating cycle in an oven at 80°C for 20 min. Various preheating cycles are reported in the literature.[12] Some authors suggest preheating the TLD-300 at 90 to 100°C for 20 to 30 min. Under these conditions we noted a significant reduction in peak 3 height, which could affect the measurement of peak 3 at very low doses (see Sec. III.B).

III.B. Sensitivity and Dose Limit for TLD-300

In a previous experiment performed in the same assembly, LiF-700 detectors were used. The results[6] showed that these detectors were unable to detect the low doses (<300 μGy) reached at the deepest experimental positions with acceptable accuracy because the background signal for LiF-700 proved to be nonnegligible or comparable to the dose to be detected. The TLD-300 can in principle operate in a more extended response dose range (up to six decades, i.e., from a few tens of micrograys to 2 Gy), but we stress that for TLDs (no matter which type), the sensitivity can be changed

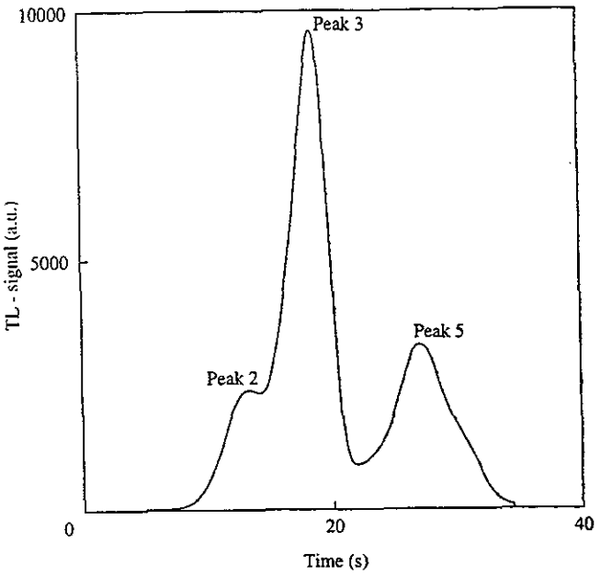

Fig. 2. Typical TL signal as a function of time for a TLD-300.

by the heating cycle, the preliminary sensitization, and the handling and the annealing procedures in use. An accurate study of the response of TLD-300 versus gamma-ray dose was performed for low- and high-level doses. The dose limits found in the present work for TLD-300 were obtained under the conditions discussed in Sec. III.A. The dose limit L_c measured for a group of k dosimeters is defined as

$$L_c = t(95\%)S_b \ , \qquad (1)$$

where $t(95\%)$ is the value of the t-student distribution (at 95% confidence level) for $k - 1$ degrees of freedom, and S_b is the standard deviation of the mean of the background signal of the detectors (measured in grays). The measurements were performed at various dose levels (down to 10 μGy) using groups of 15 detectors, and we found an averaged value $L_c = (97 \pm 35)$ μGy when the whole glow curve was measured and $L_c = (3.2 \pm 0.5)$ μGy when only peak 3 was used. The uncertainties are the standard deviation from the mean. This result gives an immediate insight into the possibility of using the TLD-300 in our experiment. Peak 3 exhibits an extremely low dose limit, ensuring that doses as low as 10 μGy can be detected with acceptable accuracy. The preceding results can be explained in terms of the background signal of the phosphor. The TL signal as a function of time, measured at 10 μGy (curve a), is compared in Fig. 3 with the background signal measured for the same detector just after the annealing cycle. It is evident that the background signal (curve b) affecting the region of interest for peak 3 (T_{max} = 150°C) is very small, while the greatest part of the background signal is produced at a higher temperature

[a]Provided by Harshaw Company.
[b]Rialto model, Vinten Company.

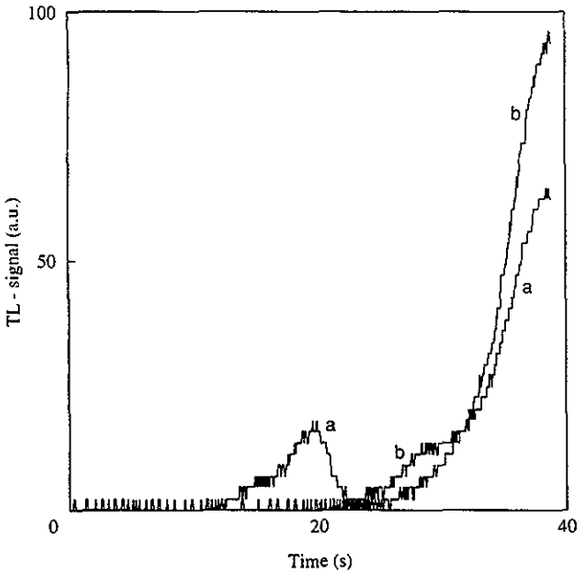

Fig. 3. The TL signal of a TLD-300 at 10 μGy compared with background signal.

(>200°C) in the region of interest for peak 5. Under these experimental conditions, we found that peak 5 cannot be properly detected for doses lower than 350 μGy (Fig. 4). At this dose level, the background correction results in about 40% of the measured signal. The background signal level also depends on the storage time of the detector after the annealing cycle.

III.C. Glow Curve Reading

As shown in Fig. 5, once the TLDs are preheated, two main peaks remain for the TLD-300. Information on the single peak can be obtained either by measuring the peak height or the peak area. In this work we used the peak area measurement as suggested in Ref. 17 when TLD-300s are used in a mixed gamma-neutron field because, due to the different responses of peaks 3 and 5 to distinct LET particles, the peak shape can be distorted.

In Fig. 5, T_M is the time at which the minimum between peaks 3 and 5 occurs, and it divides the curve into two regions. The curve to the left of T_M includes the peak 3 area (A_3), and the region to the right of T_M includes the peak 5 area (A_5). We can then write

$$A_\nu = \int_{T_a}^{T_b} I(t)\, dt \ , \qquad (2)$$

where

ν = peak 3 or peak 5

$T_a = 0$ or T_M

$T_b = T_M$ for peak 3

$T_b = T_R$ for peak 5 (where T_R is the maximum reading time in use with the chosen reading cycle)

$I(t)$ = TL signal compared with measuring time t.

In the following discussion, we will assume, in practice, that the two areas act as independent detectors.

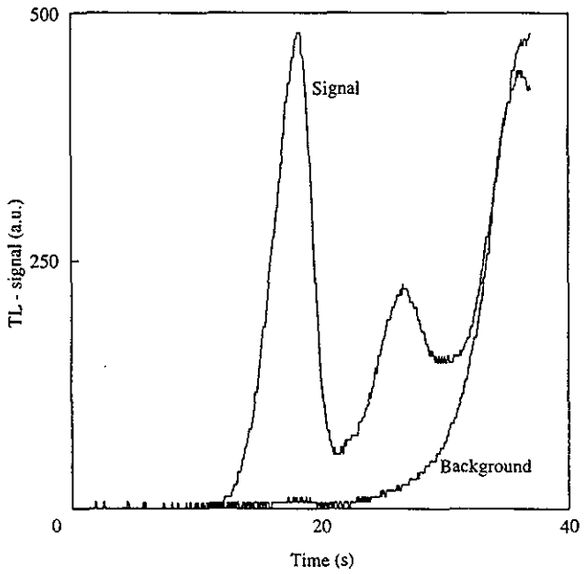

Fig. 4. The TL signal of a TLD-300 irradiated at 500 μGy compared with background signal.

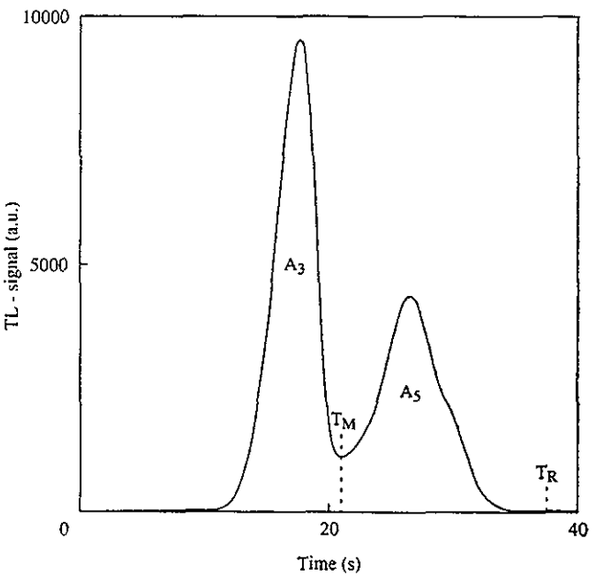

Fig. 5. The TL signal of a TLD-300 after a preheating cycle of 20 min at 80°C.

This assumption will lead to the applicability of the two-peak method to separate neutron and gamma doses. Last but not least, the use of the peak area allows the easy subtraction of the background.

III.D. Gamma-Ray Calibration

It is well known that TLD measurements do not give absolute results, and the signal (e.g., A_p) measured in the radiation field under investigation must be referred to the same quantity measured when the phosphor is irradiated by a standard gamma-ray source, typically ^{60}Co (or ^{137}Cs). The calibration was performed using the secondary standard ^{60}Co sources available from the health physics group of the Istituto Nazionale Fisica Nucleare of Laboratori Nazionali di Frascati (from 10 μGy to 350 mGy) and from the National Metrology Institute (NMI) of the ENEA Casaccia center (from 100 mGy to 35 Gy). The former secondary standards were calibrated at $\pm 10\%$ at 3σ using an ionization chamber, while the latter were calibrated at 1.5% at 3σ against a primary ^{60}Co standard source available at NMI. Note that the two calibrations overlap well, within the uncertainty, in the 100- to 350-mGy dose range.

Each calibration point was obtained by irradiating 15 detectors located in a polyethylene holder that was thick enough to allow the electronic equilibrium to be reached.

The dose in air D_{air} of ^{60}Co was converted into the TLD-300 dose D_{TLD} accounting for the μ_{en}/ρ ratio of CaF_2 to air and for the gamma-ray flux attenuation a_μ in the polyethylene holder so that

$$D_{air} = (W_{air}/e)X \tag{3}$$

and

$$D_{TLD} = [(\mu_{en}/\rho)_{TLD}/(\mu_{en}/\rho)_{air}]_{E\gamma} D_{air} a_\mu \ , \tag{4}$$

where

W_{air} = mean energy necessary to create an ion pair in air

e = electron charge

X = the known gamma-ray source exposure

$(\mu_{en}/\rho)_{TLD}/(\mu_{en}/\rho)_{air}$ = ratio of the mass energy-absorption coefficients for CaF_2 to that for air.[18]

The uncertainties of the single dose points on the calibration curve are ± 3 to 5% at 1σ (standard deviation). This total uncertainty was calculated using the quadratic propagation law and included the following contribution: the standard source intensity calibration (± 0.5 to $\pm 3.0\%$), the μ_{en}/ρ uncertainty (less than $\pm 1.5\%$), and the gamma-ray flux self-absorption in the holder ($\pm 1\%$).

The calibration was extended to 35 Gy to study the supralinear behavior of the TLD-300 because, from calculation,[6] we expected a dose of the order of 10 Gy to be reached in the experimental position close to the FNG target. The calibration was also performed for the single peaks, and we found the supralinearity to arise above ~2 Gy for peak 5, while peak 3 deviates from unity above ~14 Gy. Supralinearity seems to arise above 3 Gy for the whole TLD-300 glow curve. The measured supralinearity factors (defined as in Ref. 19) for peaks 5 and 3 are shown in Fig. 6. The experimental error is $\pm 7\%$ for each point. These results agree with similar results reported in Ref. 20. The effect produced by the observed supralinearity in our measurements is discussed in Sec. IV.C.

IV. DOSE MEASUREMENT AND CALCULATION

The TLD-300s were irradiated in nine positions inside the shielding block (in the stainless steel plates) and in six positions inside the coils (three in Type 316 stainless steel and three in copper) (see Fig. 1). In each experimental position, nine TLD-300s, housed in a Type 316 stainless steel holder (or copper holder in copper plates), were irradiated. The irradiation lasted 2.5 h, and the average neutron source intensity was 6.5×10^{10} n/s ($\pm 2\%$), measured with a silicon surface barrier detector. After the irradiation, the TLDs were preheated at 80°C for 20 min and read within 24 h of the end of the irradiation to minimize the background effect.

Since in each experimental position there were nine TLD-300s, we took the averaged TL signal and the corresponding standard deviation as measured TL response and uncertainty. This TL signal was converted to TLD dose by the calibration curve. The background signal was subtracted as well. The background was measured by 24 TLD-300s, which followed the same

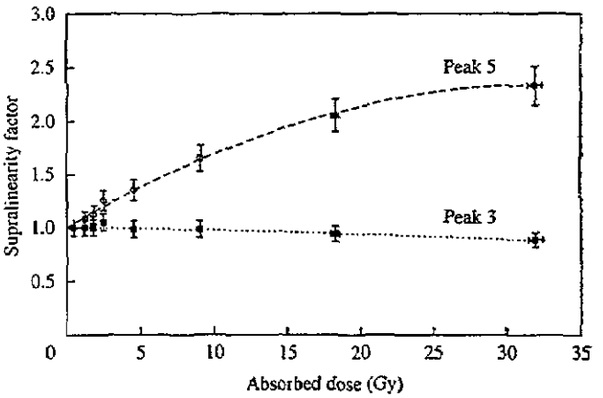

Fig. 6. Measured supralinear factors f_s as a function of absorbed dose.

history as the other TLD-300 employed for the experiment. The background contribution was not negligible for the TLDs located inside the copper-plus-stainless-steel block (coils), and it represented the main contribution to the total uncertainty (up to ±10% for peak 3 and up to ±45% for the whole area). Other uncertainties arise from the neutron source strength calibration (±2%) and fitting of the calibration points. The fitting procedure is necessary to convert the measured TL signal into dose relative to ^{60}Co (less than ±5%). For each experimental point, a total error was calculated using the quadratic propagation law.

IV.A. Monte Carlo Modeling and Calculation

The geometry of the experimental assembly and of the FNG target was modeled using the powerful geometric module of the MCNP code. The neutron source emission was modeled using an ad hoc subroutine that describes[21] the physical energy-angle-dependent neutron emission. To reduce the variance and to save computer time, the geometric model included a fine radial cell subdivision to allow the use of suitable weight windows parameters. Weight windows are based on energy-space-dependent importance functions and were self-generated in a preliminary MCNP run. The photon and neutron doses were calculated using the track length estimator multiplied by the kerma factors (the "tally 6" output of MCNP) taken from the EFF file.[5] The neutron dose includes the energy transferred by neutron reactions (n, charged particle) and by recoil nuclei. A correct interpretation of the TLD measurements requires, however, the calculation of the absorbed dose in TLD with respect to the absorbed dose in the surrounding material (stainless steel or copper), also taking into account the effects of electron transport at the interface. Because it is impractical to run an MCNP model that performs the whole calculation, including electron transport, the latter calculation was performed using a simplified model. This simplified model is composed of the TLD-300 material (CaF_2) surrounded by a sufficient volume of stainless steel (or copper). A neutron and photon surface source, calculated from the main MCNP run close to each experimental position, was applied to the boundary of the used region to get the proper electron spectrum. Reflecting boundary conditions were imposed on the electrons.

IV.B. Results

The experimental (total) absorbed dose (normalized to the neutron source strength) in CaF_2 is reported in Table I with the corresponding calculated quantities and the total uncertainty. Since the MCNP calculation gives the gamma and neutron doses in the material surrounding the detectors, in order to compare the calculation with the experimental results, the following equation was used:

$$R_{TLD} = C_p D_\gamma + C_n k_n D_n \ , \qquad (5)$$

TABLE I

Comparison Between Measured and Calculated Doses in CaF_2*

Position	Depth (cm)	Experimental	Calculated (EFF)	C/E[a]
1	2.50 SS[b]	$1.46 \times 10^{-14} \pm 6.5\%$	$1.51 \times 10^{-14} \pm 5.4\%$	1.03
2	9.51 SS	$4.31 \times 10^{-15} \pm 7.9\%$	$4.85 \times 10^{-15} \pm 5.4\%$	1.12
3	16.52 SS	$1.68 \times 10^{-15} \pm 7.7\%$	$1.83 \times 10^{-15} \pm 5.4\%$	1.09
4	23.405 SS	$7.06 \times 10^{-16} \pm 8.1\%$	$7.48 \times 10^{-16} \pm 5.4\%$	1.06
5	30.265 SS	$3.09 \times 10^{-16} \pm 8.5\%$	$2.96 \times 10^{-16} \pm 5.4\%$	0.96
6	37.08 SS	$1.19 \times 10^{-16} \pm 11.2\%$	$1.22 \times 10^{-16} \pm 5.4\%$	1.03
7	44.11 SS	$4.86 \times 10^{-17} \pm 10.6\%$	$4.49 \times 10^{-17} \pm 5.4\%$	0.92
8	50.92 SS	$1.83 \times 10^{-17} \pm 6.9\%$	$1.75 \times 10^{-17} \pm 5.8\%$	0.96
9	57.365 SS	$7.07 \times 10^{-18} \pm 10.2\%$	$6.73 \times 10^{-18} \pm 5.8\%$	0.95
10	60.62 SS	$3.19 \times 10^{-18} \pm 10.1\%$	$3.16 \times 10^{-18} \pm 6.4\%$	0.99
11	62.82 Cu[c]	$1.87 \times 10^{-18} \pm 11.2\%$	$1.78 \times 10^{-18} \pm 6.4\%$	0.95
12	65.02 SS	$1.18 \times 10^{-18} \pm 11.1\%$	$1.24 \times 10^{-18} \pm 6.4\%$	1.05
13	67.22 Cu	$8.07 \times 10^{-19} \pm 10.1\%$	$9.02 \times 10^{-19} \pm 6.4\%$	1.12
14	69.72 SS	$5.44 \times 10^{-19} \pm 12.2\%$	$6.04 \times 10^{-19} \pm 6.4\%$	1.11
15	71.62 Cu	$4.25 \times 10^{-19} \pm 14.5\%$	$6.23 \times 10^{-19} \pm 6.4\%$	1.47

*Measured in grays per neutron.
[a]Ratio of calculation to experiment.
[b]Stainless steel.
[c]Copper.

where

R_{TLD} = measured response of TLD-300 (normalized to the ^{60}Co source)

D_γ = gamma-ray absorbed dose in the surrounding material (stainless steel or copper)

D_n = neutron absorbed dose in the surrounding material (stainless steel or copper)

C_p = ratio of the photon dose in TLD to the photon dose in the material

C_n = ratio of the neutron dose in TLD to the neutron dose in the material

K_n = neutron sensitivity.

Because C_p and C_n depend on photon and neutron spectra, these ratios were calculated in each experimental position using the simplified local transport model discussed in Sec. IV.A. To obtain C_p and C_n, we run the simplified model with and without the TLD-300 material. The ratios of neutron and gamma doses in the two cases give C_n and C_p, respectively.

The calculated C_n values are reported in Table II. Their statistical uncertainty (from the calculation) was lower than ±5%. As for the C_p values, we found these to be close to unity in each experimental position within the previously claimed calculation uncertainty (±5%).

IV.C. Neutron and Gamma Dose Separation

The TLD-300 is very suitable for separating the neutron and gamma components because its two main glow peaks (peaks 3 and 5) show different sensitivities to different LET particles.[14] From Ref. 22 we know that the sensitivity of the low-temperature peak (peak 3) decreases when the LET is ~10 keV/μm, whereas the efficiency of the high-temperature peak (peak 5) stays constant up to LET values of 1000 keV/μm.

The neutron and gamma dose separation was obtained by the two-peak method.[14,15] This requires the independent measurement of the response R_ν (normalized to ^{60}Co response) for peaks 3 and 5 (Table III). The two-peak-method equations, written in a condensed form, are

$$R_\nu = D_\gamma^* + k_\nu D_n^* , \quad (6)$$

where D_n^* and D_γ^* refer to the absorbed dose in the dosimeter, and we have

$$D_n^* = C_n D_n \quad \text{and} \quad D_\gamma^* = C_p D_\gamma . \quad (7)$$

The symbols have the same meaning as in Eq. (5) (ν represents the peak number 3 or 5). Equation (6) shows the different sensitivities of peaks 3 and 5 to neutrons via the k_ν term.

In Table III, where the R_3 and R_5 as well as the R_{TLD} (i.e., using the whole glow curve) responses are

TABLE II

Experimental and Calculated Results for C_n and γ and Neutron Absorbed Doses*

Depth (cm)	D_γ/D_{TLD}	Measured D_γ[a]	Calculated D_γ[b]	C/E[c]	C_n	Measured D_n[a]	Calculated D_n[b]	C/E
2.50 SS[d]	0.70	1.24×10^{-14}	1.30×10^{-14}	1.05	3.44	5.66×10^{-15}	5.49×10^{-15}	0.97
9.51 SS	0.83	4.04×10^{-15}	4.61×10^{-15}	1.14	3.54	1.01×10^{-15}	9.21×10^{-16}	0.91
16.52 SS	0.89	1.61×10^{-15}	1.78×10^{-15}	1.11	3.50	3.31×10^{-16}	2.30×10^{-16}	0.70
23.405 SS	0.92	6.88×10^{-16}	7.35×10^{-16}	1.07	3.45	8.74×10^{-17}	6.60×10^{-17}	0.76
30.265 SS	0.93	3.05×10^{-16}	2.92×10^{-16}	0.95	3.43	1.28×10^{-17}	2.08×10^{-17}	1.62
37.08 SS	0.94	1.12×10^{-16}	1.20×10^{-16}	1.07	3.48		8.31×10^{-18}	
44.11 SS	0.95	4.04×10^{-17}	4.45×10^{-17}	1.10	3.53		2.29×10^{-18}	
50.92 SS	0.96	1.10×10^{-17}	1.74×10^{-17}	1.58	3.58		7.85×10^{-19}	
57.365 SS	0.95		6.67×10^{-18}		3.62		3.29×10^{-19}	
60.62 SS	0.94		3.12×10^{-18}		3.77		2.01×10^{-19}	
62.82 Cu[e]	0.96		1.67×10^{-18}		6.73		6.70×10^{-20}	
65.02 SS	0.92		1.22×10^{-18}		3.86		9.14×10^{-20}	
67.22 Cu	0.95		8.43×10^{-19}		7.24		4.88×10^{-20}	
69.72 SS	0.90		5.92×10^{-19}		3.93		6.35×10^{-20}	
71.62 Cu	0.96		5.84×10^{-19}		7.51		2.69×10^{-20}	

*Measured in grays per neutron.
[a]Experimental uncertainty is ±30%.
[b]Statistical uncertainty is ±5% for the MCNP calculation.
[c]Ratio of calculation to experiment.
[d]Stainless steel.
[e]Copper.

TABLE III

Measured R_ν and R_{TLD} Responses Normalized to the ^{60}Co Gamma-Ray Source

Depth (cm)	R_3 (Gy)	R_5 (Gy)	R_{TLD} (Gy)
2.50 SS[a]	9.38 ± 6.2%	17.75 ± 6.5%	12.90 ± 6.3%
9.51 SS	2.78 ± 7.6%	3.73 ± 7.3%	3.17 ± 7.6%
16.52 SS	1.09 ± 7.4%	1.21 ± 7.5%	1.13 ± 7.3%
23.405 SS	4.56×10^{-01} ± 7.8%	4.82×10^{-01} ± 8.1%	4.60×10^{-01} ± 7.8%
30.265 SS	2.00×10^{-01} ± 8.3%	2.04×10^{-01} ± 9.5%	1.95×10^{-01} ± 8.3%
37.08 SS	7.71×10^{-02} ± 11.0%	8.91×10^{-02} ± 12.5%	7.53×10^{-02} ± 10.4%
44.11 SS	3.14×10^{-02} ± 10.4%	4.51×10^{-02} ± 15.0%	3.14×10^{-02} ± 10.0%
50.92 SS	1.18×10^{-02} ± 6.6%	2.43×10^{-02} ± 25.0%	1.14×10^{-02} ± 8.5%
57.365 SS	4.56×10^{-03} ± 10.0%		4.58×10^{-03} ± 8.5%
60.62 SS	2.06×10^{-03} ± 10.0%		2.08×10^{-03} ± 13.0%
62.82 Cu[b]	1.21×10^{-03} ± 11.0%		1.27×10^{-03} ± 13.0%
65.02 SS	7.64×10^{-04} ± 11.0%		7.84×10^{-04} ± 23.0%
67.22 Cu	5.21×10^{-04} ± 10.0%		5.02×10^{-04} ± 30.0%
69.72 SS	3.51×10^{-04} ± 11.0%		3.86×10^{-04} ± 35.5%
71.62 Cu	2.74×10^{-04} ± 11.3%		3.34×10^{-04} ± 51.5%

[a]Stainless steel.
[b]Copper.

listed, the data indicate that the responses of the two main peaks agree, within the errors, for the dosimeters located inside the block at penetration depth $z > 25$ cm. Table III also shows the supralinearity response for peak 5 and for R_{TLD} in the first three experimental positions (see the dose limit discussed in Sec. III.B). In the case of supralinear response, Eq. (6) can be solved by introducing the supralinear factors f_ν for each single peak ν setting $D_\nu^* = f_\nu D_\nu^\circ$ for both gammas and neutrons. As for the neutron dose D_n^*, we know from Ref. 19 that the supralinear effect caused by the neutron dose rises above 100 Gy for TLD-300. Since 100 Gy of neutron dose is more than can be obtained in our experiment, in this work we assumed that the neutron response is linear with the dose ($D_n^* \equiv D_n^\circ$). If we use the supralinearity factors only for the gamma absorbed dose, putting $D_\gamma^* = f_\nu D_\gamma^\circ$ into Eq. (6), and solve for D_n° and D_γ°, we obtain

$$D_\gamma^\circ = \frac{\left(R_5 - \frac{k_5}{k_3} R_3\right)}{\left(f_5 - f_3 \frac{k_5}{f_3}\right)} \tag{8}$$

and

$$D_n^\circ = \frac{(f_5 R_3 - f_3 R_5)}{(f_5 k_3 - f_3 k_5)} . \tag{9}$$

In this work we always have $f_3 = 1$ for all the experimental positions because $f_3 < 1$ for $D^* > 15$ Gy. Note that when the TLD-300 is working in the linear response range (i.e., below 2 Gy), $f_5 = 1$, and Eqs. (7) and (8) become the straightforward solution of the two-peak method.

Using Eqs. (8) and (9) and accounting for Eqs. (7), we obtain the experimental gamma and neutron doses in the materials that are reported in Table II, where they are also compared with the MCNP-calculated quantities.[6] The experimental results for D_γ and D_n are affected by large uncertainties (±20 and ±30%, respectively), mainly due to k_3 and k_5, which are known[23] at ±20%. As already stated in Sec. III.D, the uncertainty affecting f_ν is ±7%. It is evident that the results agree within the uncertainties for both D_γ and D_n. The gamma dose is measured throughout the first block, while the results for D_n refer to the first five positions inside the Type 316 stainless steel plus water shield. The neutron dose varies from ~30% of the total in the first experimental position, down to <7% of the total dose at 30 cm inside the shield. From this point onward, the nuclear heating is mainly due to gamma-ray production.

V. DISCUSSION

Apart from the supralinearity factors, Eqs. (8) and (9) depend on the difference between R_3 and R_5. When the magnitude of the D_γ/D_{TLD} ratio is close to unity (i.e., for depth >25 cm, see Table III), $R_{TLD} \approx R_3$. Since the neutron dose is very low (≤7%) and peak 3 is scarcely sensitive to neutrons, the dose measured using peak 3 can be assumed (with an error ≤7%) to

be the gamma-ray dose in the deepest positions of the shield and in the superconducting coils. This allows one to determine the absorbed dose accurately because peak 3 shows a very low dose detection limit, while the measured total area shows a larger background effect that reduces the accuracy of the measurement (Table II). Thus, in deep positions, the neutron absorbed dose can be obtained only by calculation.

Equations (8) and (9) also depend on the k_v parameter, and a discussion is necessary about the used data. We know from Ref. 23 that the neutron sensitivity of the two main peaks of TLD-300 varies with neutron energy. In our experiment we have a strong variation of the neutron field (due to the shielding performance of the experimental assembly) going from positions close to the target to the deepest positions inside the coils. To account for this variation, the data available[23] for a comparison of the TLD-300 neutron sensitivity and the neutron energy $[k_v(E)]$ were fitted, collapsed into group structure using (g is the group index)

$$k_v^g = \frac{\int_{E_g}^{E_{g+1}} k_v(E)\,dE}{\int_{E_g}^{E_{g+1}} d(E)}\,, \tag{10}$$

and thus weighted for each experimental position j over the neutron flux spectrum ϕ_g^j obtained from the MCNP calculation (NG energy groups):

$$k_v^j = \frac{\sum_1^{NG} k_v^g \cdot \phi_g^j}{\sum_1^{NG} \phi_g^j}\,. \tag{11}$$

The calculated k_v^j values are shown in Fig. 7. We stress that the data used for the fitting procedure are in the 1- to 14-MeV neutron energy range. From literature[16] we know that TLD-300s are suitable for separating the neutron and gamma doses at high neutron energies, and it was demonstrated[15] that TLD-300s become rather inapplicable when the neutron energy decreases (e.g., reactor spectrum). In this work we found a similar result, because for neutron spectrum average energy <1 MeV, which corresponds to position 5 in our experimental assembly (Fig. 7), we cannot separate the neutron and gamma doses.

The method used in this work to separate the neutron and gamma doses has some drawbacks because the parameters to be used in Eq. (5) (k_v, C_p and C_n) are weighted over the calculated neutron spectrum. This introduces a correlation between the calculation to be tested and the experiment. The problem can be overcome for k_v by measuring these values in the experimental positions. The feasibility of this experiment is under consideration. As far as the C_p and the C_n values are concerned, although they depend on the neutron and gamma energy spectra, it was clearly shown in Sec. IV and Table II that they do not vary much in our assembly between the first (hard spectrum) and the last (soft spectrum) experimental positions. The value C_n can also be calculated from tabulated kerma values, while C_p can be set equal to unity (see Sec. IV) with very good approximation. As far as we know, there are no other methods based on the use of TLD that allow for neutron and gamma dose separation without a drawback. The method proposed in Ref. 11 is suitable for obtaining the gamma dose in a pure gamma field, but in a mixed neutron and gamma field, it requires the neutron spectrum to substract the neutron contribution because the different TLDs to be used have different neutron sensitivities and thus different responses to the same neutron dose. This fact must be accounted for before performing the interpolation to obtain the gamma dose.

VI. CONCLUSION

For the first time, TLD-300 dosimeters have been used to measure nuclear heating in a shielding block simulating the shield of a next-step fusion reactor. The use of the TLD-300 allowed measurement of the absorbed dose in a wide range from a few tens of micrograys to 10 Gy. Using the peak area and measuring peaks 3 and 5 separately, after proper calibration and background subtraction, the lowest doses were measured with a total error less than ±15%. This result allowed, even in the deepest position inside the superconducting coils, an accurate comparison with the doses calculated by the MCNP code using the EFF. For

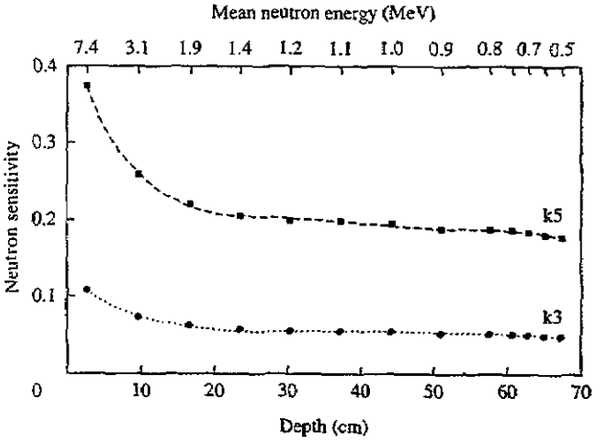

Fig. 7. Neutron sensitivity k_v for peaks 5 and 3 of the TLD-300 averaged over the calculated neutron spectrum in each experimental position. The upper horizontal axis reports the mean neutron flux energy calculated from the MCNP spectra given in Ref. 6.

the first time, in tokamak shielding experiments, the neutron absorbed dose was experimentally separated from the gamma absorbed dose using the two-peak method. These results show that the neutron contribution to the total absorbed dose is <30% also in positions close to the neutron source, and the D_n contribution is negligible with respect to the D_γ contribution in the superconducting coils. The experimental neutron doses agree rather well with the calculated ones (using the kerma values from the EFF dosimetric file) in the first two experimental positions, while the difference grows up to 30% for detectors located 25 cm inside the block. Until now, TLD-300s were used in health physics studies to separate neutron and gamma doses; this work has proven the applicability of the TLD-300s and of the two-peak method to separate neutron and gamma doses even in tokamak shielding experiments. However, the accuracy achieved for neutron dose discrimination in this study is not yet satisfactory. It can be further improved by reducing the uncertainty for the neutron sensitivities of peaks 3 and 5. This requires further effort for the in-spectrum measurement of these data. This work has also confirmed the already claimed limit for the applicability of TLD-300 for neutron and gamma dose discrimination as the neutron energy decreases.

REFERENCES

1. P. H. REBUT, "ITER, The First Experimental Fusion Reactor," *Fusion Eng. Des.*, **30**, 85 (1995).

2. M. MARTONE, M. ANGELONE, and M. PILLON, "The 14 MeV Frascati Neutron Generator," *J. Nucl. Mater.*, **212–215**, 1661 (1994).

3. A. C. LUCAS and B. M. KAPSAR, "The Thermoluminescence of Thulium Doped Calcium Fluoride," *Proc. Fifth Int. Conf. Luminescence Dosimetry*, Sao Paulo, Brazil, February 14–17, 1977, p. 131 (1977).

4. "MCNP, A General Monte Carlo N-Particle Transport Code, Version 4-A," LA 12625-M, L. BRIESMEISTER, Ed., Los Alamos National Laboratory (Nov. 1993).

5. H. GRUPPELAAR, "Status of the European Fusion File (EFF/2)," EFF-DOC-17, Nuclear Energy Agency (July 1988).

6. P. BATISTONI et al., "Nuclear Heating Experiments for the Validation of the Fusion Reactor Shielding Performance," *Fusion Eng. Des.* (to be published).

7. M. KRIENS, R. SCHMIDT, A. HESS, and W. SCOBEL, "Calibration Methods of TLD-300 Dosimeters in a Clinical 14 MeV Neutron Beam," *Radiat. Prot. Dosim.*, **44**, *1/4*, 309 (1992).

8. W. HOFFMAN and P. SONSIRIRITTHIGUL, "TLD-300 Dosimetry at Chiang Mai 14 MeV Neutron Beam," *Radiat. Prot. Dosim.*, **44**, *1/4*, 301 (1992).

9. J. BENVENISTE, H. C. MITCHELL, C. A. SCHRADER, and J. H. ZENGER, "The Problem of Measuring the Absolute Yield of 14 MeV Neutrons by Means of an Alpha Counter," *Nucl. Instrum. Methods*, **7**, 306 (1960).

10. M. ANGELONE, M. PILLON, P. BATISTONI, M. MARTINI, M. MARTONE, and V. RADO, "Absolute Experimental and Numerical Calibration of the 14 MeV Neutron Source at the Frascati Neutron Generator," *Rev. Sci. Instrum.*, **67**, *6*, 2189 (1996).

11. S. TANAKA and N. SASAMOTO, "Gamma Ray Absorbed Dose Measurements in Media with Plural Thermoluminescent Dosimeters Having Different Atomic Numbers," *J. Nucl. Sci. Technol.*, **22**, *2*, 109 (1985).

12. C. FURETTA and Y.-K. LEE, "Annealing and Fading Properties of CaF2:Tm (TLD-300)," *Radiat. Prot. Dosim.*, **5**, *1*, 57 (1983).

13. A. J. J. BOS and J. B. DIELHOF, "The Analysis of Thermoluminescent Glow Peaks in CaF2:Tm (TLD-300)," *Radiat. Prot. Dosim.*, **37**, *4*, 231 (1991).

14. A. C. LUCAS and B. M. KAPSAR, "Heavy Particle Dosimetry with High Temperature Peaks of CaF_2:Tm and ^{7}LiF Phosphors," *Radiat. Prot. Dosim.*, **6**, 149 (1983).

15. M. APOSTOLOVA, G. BURGER, D. COMBECHER, H. ECKERL, and P. KNEUSCHAUREK, "The Use of TLD Detectors for Reactor Mixed Dosimetry," *Proc. 5th Symp. Neutron Dosimetry—Beam Dosimetry*, Munich/Neuherberg, Germany, September 17–21, 1984, EUR 9762 EN, p. 817, Commission of the European Communities (1985).

16. J. RASSOW et al., "Spectral Dependence of Response Coefficients and Applicability of the Two-Peak TLD Method in Mixed Neutron-Photon Radiation Field," *Proc. 5th Symp. Neutron Dosimetry-Beam Dosimetry*, Munich/Neuherberg, Germany, September 17–21, 1984, EUR 9762 EN, p. 783, Commission of the European Communities (1985).

17. J. A. B. GIBSON, "The Relative Tissue-Kerma Sensitivity of Thermoluminescent Materials to Neutrons," EUR 10105 EN, Commission of the European Communities (1985).

18. J. H. HUBBEL, "Photon Mass Attenuation and Energy Absorption Coefficients from 1 keV up to 20 MeV," *Int. J. Appl. Radat. Isot.*, **33**, 1269 (1982).

19. Y. HOROWITZ, *Thermoluminescence and Thermoluminescent Dosimetry*, Vol. II, p. 1, CRC Press, Boca Raton, Florida (1984).

20. J. RASSOW, C. CLEIN, and P. MEISSNER, "Supralinearity Behaviour of TLD-300 and TLD-700," *Radiat. Prot. Dosim.*, **23**, *1/4*, 409 (1988).

21. M. PILLON, M. ANGELONE, M. MARTONE, and V. RADO, "Characterization of the Source Neutrons Produced by the Frascati Neutron Generator," *Fusion Eng. Des.*, **28**, 683 (1995).

22. W. HOFFMANN and G. MOLLER, "Heavy Particle Dosimetry with High Temperature Peaks of Thermoluminescent Materials," *Nucl. Instrum. Methods*, **175**, 205 (1980).

23. J. B. DIELHOF, A. J. J. BOS, J. ZOETELIEF, and J. J. BROERSE, "Sensitivity of CaF_2 Thermoluminescent Materials to Fast Neutrons," *Radiat. Prot. Dosim.*, **23**, *1/4*, 405 (1988).